ACES Asian Chemical Editorial Society

DOI: 10.1002/cnma.201700081

CHEMNANOMAT
Full Paper

Thermoresponsive Systems

# Measuring Temperature Change at the Nanometer Scale on Gold Nanoparticles by Using Thermoresponsive PEGMA Polymers**

Mustafa S. Yavuz,*[a] Murat Citir,*[b] Halit Cavusoglu,[c] and Gokhan Demirel*[d]

**Abstract:** Plasmonic heating of gold nanoparticles (AuNPs) under laser illumination is a highly desirable technique, especially for cancer therapy. However, significant drawbacks still remain including uncontrolled heat release from AuNPs, random exposure duration, and selection of the proper laser power without damaging normal healthy cells. Herein, we demonstrate a simple and versatile method to measure temperature variation on the surface of Au nanoparticles under laser irradiation based on a thermoresponsive polymer, poly(ethylene glycol) methylether methacrylate (PEGMA). In this context, a series of PEGMA polymers were synthesized to have different lower critical solution temperature (LCST) values (28–90 °C) and conjugated to the surface of spherical AuNPs by a gold–thiolate linkage. According to our strategy, the AuNPs first photothermally absorb light energy and convert it to heat owing to their tailored photothermal characteristics. The generated heat from the AuNPs subsequently dissipates into the surrounding thermoresponsive PEGMA polymer. When the temperature generated on the Au surface upon laser irradiation for a certain exposure time reaches the LCST value of the surrounding PEGMA polymer, the polymer chain collapses. Therefore, the hydrodynamic diameter of the PEGMA-coated AuNPs changes, which can be easily monitored by using dynamic light scattering (DLS). We systematically measured the temperature (28–90 °C) generated on the AuNP surfaces by using different laser power densities with varying durations. We believe that the resulting strategy will be very valuable for oncologists to easily predict the minimum laser power and duration needed to destroy the cancer cells through the photothermal effect of Au nanostructures.

## Introduction

Gold nanoparticles (AuNPs) have emerged as ideal tools for various medical and non-medical applications including photothermal therapy,[1] drug delivery,[2] cancer diagnosis,[3] organic reactions and polymerizations,[4] thermal degradation,[5] and plasmon-mediated heating,[6] as they possess easy functionalization, inertness, non-toxicity, and tunable localized surface plasmon resonances (LSPR).[7] Among the medical applications of AuNPs, photothermal cancer therapy, which is based on converting light to heat energy by AuNPs, has recently come into prominence. In this context, several promising works have been done.[8] For example, the anti-epidermal growth factor receptor antibody conjugated 40 nm AuNPs were used to destroy the malignant cancer cells upon exposure of a 514 nm continuous laser at different power densities between 13 and 64 W cm$^{-2}$ for 4 min.[9] In another study, antibody-conjugated 20 nm AuNPs added to mature murine macrophage cells, which were successfully destroyed after irradiation with a 543.5 nm green HeNe laser with a power of approximately 2.5 mW for 10 min.[10]

Besides medical applications of photothermal AuNPs, there has been great interest in the non-medical areas. For instance, plasmonic heating of AuNPs inside polydimethylsiloxane (PDMS) was applied for thermal curing at the nanoscale to generate a PDMS shell (80–430 nm) within 16 seconds under 532 nm continuous wave (CW) laser irradiation with a power density of 378 kW cm$^{-2}$.[11] In another work, polyurethane films were photothermally cured from isocyanide and alcohol reactants in bulk-scale in the presence of 2 nm AuNPs under 532 nm Nd:YAG pulsed laser (8 ns pulses, 50 mJ pulse$^{-1}$) irradi-

[a] Prof. M. S. Yavuz
Department of Metallurgy and Materials Engineering
Selcuk University
42075, Konya (Turkey)
E-mail: selmanyavuz@gmail.com

[b] Prof. M. Citir
Materials Science and Nanotechnology Engineering
Abdullah Gül University
38080, Kayseri (Turkey)
E-mail: muratcitir@gmail.com

[c] Dr. H. Cavusoglu
Department of Physics
Selcuk University
42075, Konya (Turkey)

[d] Prof. G. Demirel
Bio-inspired Materials Research Laboratory
Department of Chemistry
Gazi University
06500, Ankara (Turkey)
E-mail: nanobiotechnology@gmail.com

[**] PEGMA = poly(ethylene glycol) methylether methacrylate

Supporting information and ORCID(s) from the author(s) for this article are available on the WWW https://doi.org/10.1002/cnma.201700081.

ation at 12.5 mW cm$^{-2}$ for 4 min, which resulted a billion-fold enhancement of curing rate.[12] In addition, interfacial damage on a glass fiber was photothermally healed and interlocked by melting 40–120 μm PMMA (poly(methyl methacrylate)) resins in the presence of AuNPs with 1600 W cm$^{-2}$ power density of 532 nm CW diode laser irradiation for 5 min.[13] Recently, we also demonstrated a photothermal degelation of AuNPs embedded peptide organogels within 10 seconds by irradiating with a 532 nm green laser at a power density of 50 mW cm$^{-2}$.[14] Although all these photothermal applications were successfully demonstrated by using AuNPs, however, these still suffer from random laser exposure durations using various laser powers to reach such temperatures. To this extent, besides the use of traditional thermometer devices, the temperature of a solution containing AuNPs upon laser irradiation is usually measured by using thermal camera systems.[15] However, measuring the temperature change of the heated solution by thermal camera or digital thermometers is limited to high AuNP concentrations in the macroscale. Therefore, the temperature change (or the heat released) from the surface of the AuNPs needs to be precisely measured at the nanoscale to standardize (or eventually lower) the laser irradiation exposure times.

In recent years, the temperature measurement at the nanoscale has been utilized by using rare-earth metal nanoparticles, quantum dots, biomolecules, and organic fluorophores.[16] Among these, the heat released on AuNP surfaces upon laser irradiation was mostly measured by fluorescent (optical) thermometers, which are based on an increment in fluorescence emission during fluorescent molecule release from the Au surface.[17] Although these optical methods have great sensitivity towards thermal sensing at the nanoscale, the strong quenching effect of gold, expensive and complex synthesis of thermometer material, and measuring only a narrow temperature range are the main obstacles to overcome. To the best of our knowledge, there is still no such simple and non-optical technique using easily synthesized and inexpensive platforms for measuring the wide range of temperatures generated on the AuNP surfaces at the nanoscale. In this study, we demonstrate a simple and facile strategy to measure the temperature change (28–90 °C) on the surface of AuNPs during a photothermal process by using a thermoresponsive polymer.

## Results and Discussion

To calculate the temperature variation at AuNP surfaces at the nanoscale, the hydrodynamic diameters of AuNPs coated with poly(ethylene glycol) methyl ether methacrylate (PEGMA@AuNPs) were recorded by using a dynamic light scattering (DLS) instrument before and after light illumination. As shown schematically in Figure 1a, when the AuNP generates heat under light illumination as a result of the photothermal effect, the thermoresponsive PEGMA coating on the AuNP surface shrinks after reaching the polymer's lower critical solution temperature (LCST). This shrinkage or conformational change of the PEGMA polymer on AuNPs will dramatically reduce the average hydrodynamic size of these nanoparticles, which indicates a specific temperature change on the AuNPs at the nanoscale.

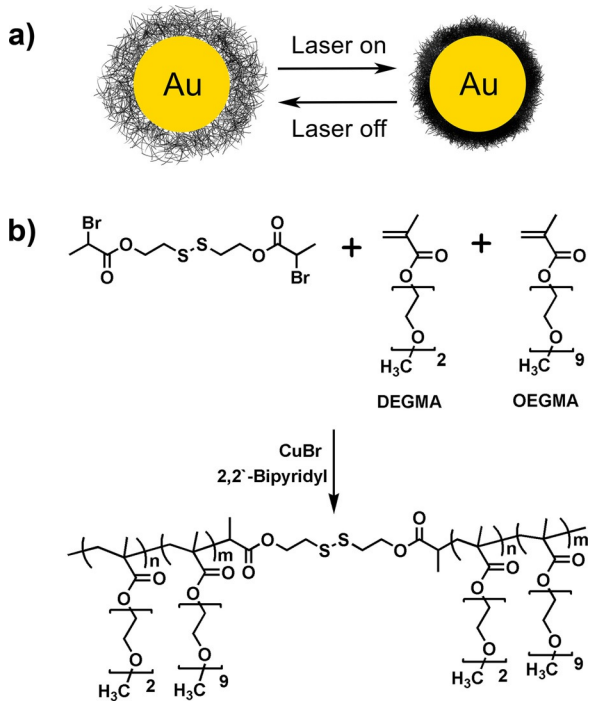


**Figure 1.** (a) The schematic illustration of the change in size of PEGMA@AuNPs under laser irradiation. (b) Synthesis of the disulfide-containing thermosensitive PEGMA polymer by atom-transfer radical polymerization (ATRP) as initiated by a disulfide initiator in the presence of a $Cu^{I}$ catalyst.

In this work, the thermoresponsive PEGMA polymer was covalently bonded to the surface of the Au nanoparticles (AuNPs) by a gold–thiolate linkage. As shown in Figure 1b, the PEGMA polymer was first synthesized by using a disulfide initiator that resulted in a disulfide bond in the middle of the corresponding polymer. The initiator was synthesized by the esterification reaction of 2-bromopropionic acid and 2-hydroxyethyl disulfide according to the previously reported procedure.[18] Two monomers, diethylene glycol methyl ether methacrylate (DEGMA) and oligo(ethylene glycol) methyl ether methacrylate (OEGMA), were used to tune the LCST of the PEGMA polymers. PEGMA polymers with LCST values of 28, 32, 37, 39, 49, 59, 69, 79, and 90 °C were synthesized by using different DEGMA/OEGMA ratios.[19] The aqueous solution of hydrophilic PEGMA polymer with an LCST of 39 °C is transparent at room temperature (below LCST) and a cloudy white solution at 41 °C (above LCST; Figure 2a). After cooling, the cloudy solution turned clear again owing to a reversible coil-to-globule transition.[20]

The phase transformation of the PEGMA polymer was measured with a UV/Vis spectrophotometer. For the PEGMA polymer transitions at different LCSTs, the UV/Vis data are plotted as transmittance versus temperature. When the OEGMA monomer (the longer PEG chain) content of the corresponding polymer was increased, the LCST of the polymer was expected to shift to a higher LCST value. The LCST value of each PEGMA polymer was calculated from the transmittance graph (Fig-

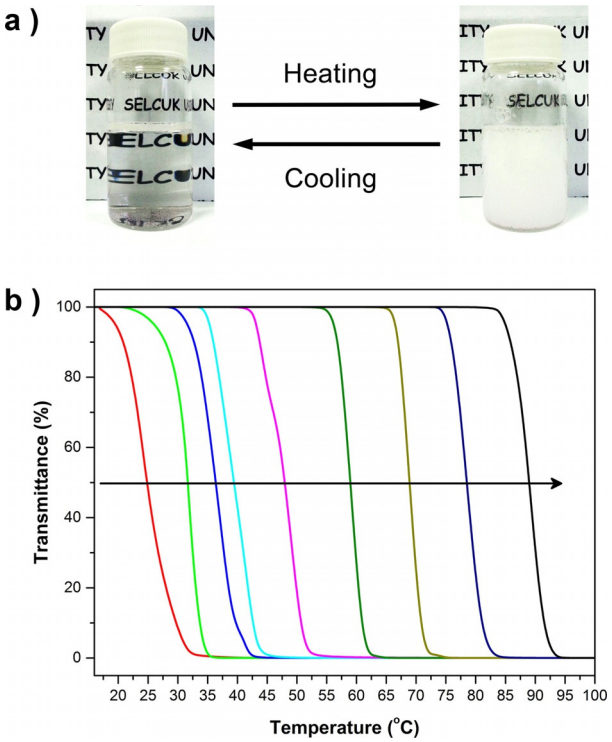


**Figure 2.** (a) LCST behavior of PEGMA below and above LCST. (b) Plots of transmittance as a function of temperature (450 nm, 1 °C min$^{-1}$) measured for aqueous solutions of PEGMA polymers.

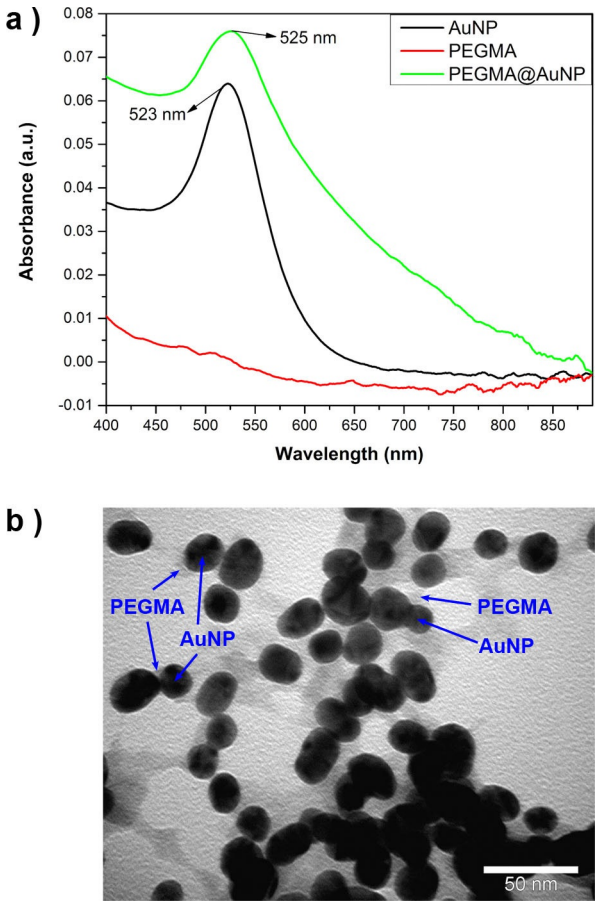


**Figure 3.** (a) UV/Vis absorption spectra for AuNP, PEGMA, and PEGMA@AuNP. (b) TEM image of PEGMA@AuNPs.

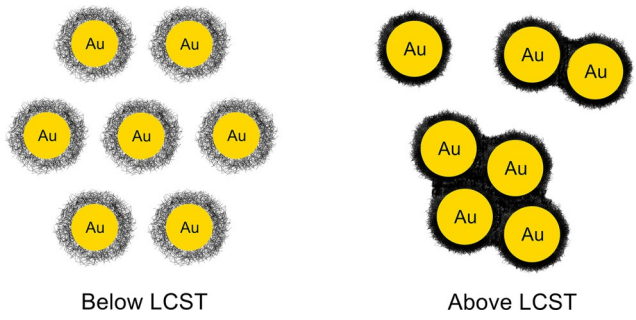


**Figure 4.** Illustration of aggregation of PEGMA@AuNPs.

ure 2 b) and visually confirmed by the appearance of cloudiness upon conventional heating. The surface plasmon resonance (SPR) peak of as-synthesized citrate-coated AuNPs occurs at 523 nm (Figure 3 a). The bare PEGMA polymer is transparent in the UV/Vis region. After the conjugation of PEGMA polymer to AuNPs, the SPR peak was redshifted by approximately 2 nm, which confirms the displacement process between the citrate and thiolate groups on the PEGMA polymer. After conjugating citrate-coated AuNPs with PEGMA polymers, the AuNPs were covered by a thin polymer layer, as observed in TEM images (Figure 3 b). Moreover, the similarities in FTIR spectra of PEGMA@AuNPs and bare PEGMA also confirm the successful conjugation of PEGMA polymer on the AuNP surfaces (Figure S1 in the Supporting Information).

Before measuring the temperature change on the AuNP surface upon laser irradiation, we heated the aqueous solution of PEGMA@AuNPs (LCST = 37 °C) conventionally by using a heating unit attached to the DLS equipment. Prior to heating, the hydrodynamic diameter of the PEGMA@AuNPs was measured to be approximately 52 nm at 25 °C (below LCST). For each 1 °C increase in the temperature, the hydrodynamic diameter of the PEGMA@AuNPs was recorded. When the temperature of the solution reached 37 °C, the hydrodynamic diameter initially dropped to approximately 43 nm. However, it suddenly started to increase in an irrelevant way and reached 201 nm. This could be due to the aggregation of hydrophobic PEGMA polymers above the LCST (Figure 4) as a similar result was reported in the literature.[21] This size change of the PEGMA@AuNPs confirms that the thermoresponsive behavior of PEGMA on AuNPs was still functional after conjugation. For comparison, we also prepared AuNPs conjugated with polyvinyl pyrrolidone (PVP), which is not a thermoresponsive polymer, and the same heating procedure was applied to the PVP@AuNPs solution. As expected, we did not observe any notable change in the hydrodynamic diameter. At room temperature, the size of PVP@AuNPs was approximately 64 nm, whereas it only decreased to 62 nm after heating to 50 °C.

The results for measuring the change in hydrodynamic diameter of the PEGMA@AuNPs during conventional heating enable one to measure the temperature on the surface of

AuNPs by laser irradiation. We investigated the photothermal effects of AuNPs with an LSPR peak of 525 nm upon laser irradiation by using a 532 nm tunable continuous-wave (CW) laser (0.1–2.5 W). The hydrodynamic diameter of the PEGMA@AuNPs was recorded after each laser irradiation. Five different CW laser powers of 2.5, 1, 0.5, 0.25, and 0.1 W, which correspond to power densities of 1.88, 0.753, 0.377, 0.188, and 0.075 W cm$^{-2}$, respectively, were applied. Every 3 seconds, the average hydrodynamic diameter of the solution was recorded for each laser irradiation trial. After 5 min, we increased the time interval between recordings of DLS measurements to 1 min intervals for 20 min and then 5 min intervals. If there was no change in the hydrodynamic diameter of the PEGMA@AuNPs after 45 min of laser exposure, we stopped analyzing the size change. It should be noted that the OEGMA or DEGMA (used to tune LCST of PEGMA) content does not affect the thermal transport rate, and, thus, the time listed in Table 1 and plotted in Figure 5.

**Table 1.** Times required to change the hydrodynamic diameter when PEGMA@AuNPs with different LCST values were exposed to different laser powers. The OEGMA (used to tune LCST of PEGMA) content does not affect the thermal transport rate, not affecting the time listed in Table 1 and plotted in Figure 5.

| LCST [°C] | 1.88 [W cm$^{-2}$] | 0.753 [W cm$^{-2}$] | 0.377 [W cm$^{-2}$] | 0.188 [W cm$^{-2}$] | 0.075 [W cm$^{-2}$] |
|---|---|---|---|---|---|
| 28 | < 3 s | < 3 s | < 3 s | < 3 s | 3 s |
| 32 | 3 s | 12 s | 35 s | 150 s | 420 s |
| 37 | 10 s | 25 s | 60 s | 180 s | 600 s |
| 39 | 20 s | 30 s | 150 s | 300 s | 900 s |
| 49 | 30 s | 45 s | 240 s | 420 s | 1200 s |
| 59 | 45 s | 90 s | 330 s | 450 s | –[a] |
| 69 | 70 s | 300 s | 1050 s | 1800 s | –[a] |
| 79 | 180 s | 900 s | –[a] | –[a] | –[a] |
| 90 | 45 min | –[a] | –[a] | –[a] | –[a] |

[a] No change in hydrodynamic diameter of the PEGMA@AuNPs after 45 min of laser exposure.

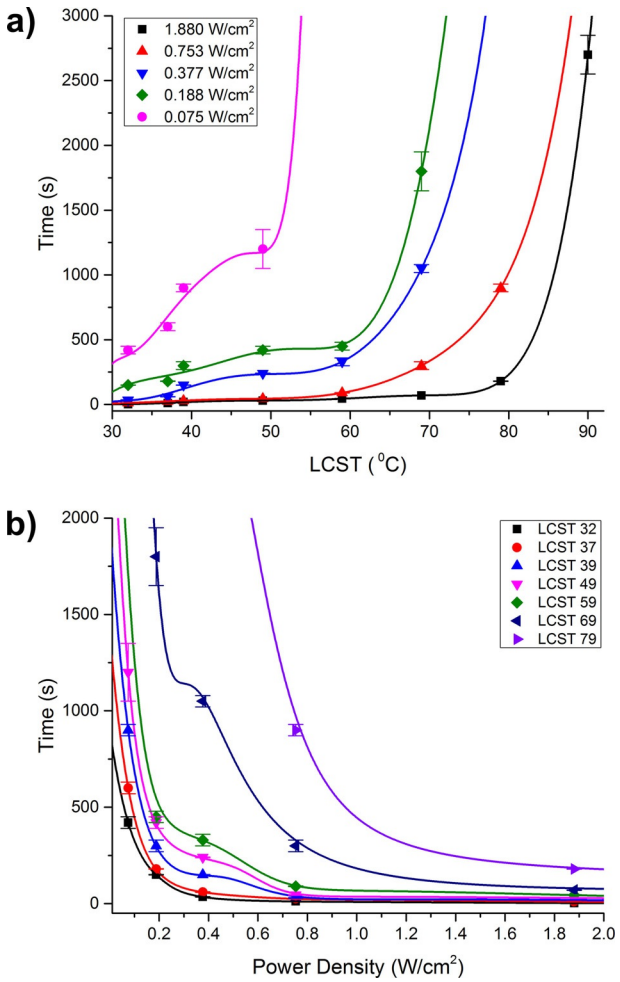


**Figure 5.** (a) Time versus different LCST values of PEGMA@AuNPs with respect to the laser power density. Solid lines are high precision seventh-order polynomial function fits to the experimental data. (b) Time versus power density with respect to the LCST values of PEGMA@AuNPs. Solid lines are quintic/quintic rational function fits to the experimental data.

To find the shortest and longest treatment duration needed to reach the corresponding LCST temperature on the PEGMA@AuNPs, we first applied a laser power density of 1.88 W cm$^{-2}$ (highest) and 0.075 W cm$^{-2}$ (lowest) to each of the solutions with different LCST values. In the case of PEGMA@AuNPs with an LCST of 28 °C (hereafter referred to as PEGMA28@AuNPs), the time required for the hydrodynamic diameter change of the PEGMA28@AuNPs was less than 3 seconds (i.e., immediately) for 1.88 W cm$^{-2}$ and only 3 seconds for 0.075 W cm$^{-2}$, as shown in Table 1.

Afterwards, we irradiated the PEGMA@AuNPs solution with the highest LCST value of 90 °C (PEGMA90@AuNPs). In this case, we first applied the highest laser power density (1.88 W cm$^{-2}$) to this solution. Upon 45 min laser exposure, we observed a change in the hydrodynamic diameter of PEGMA90@AuNPs. Hence, to reach 90 °C on the AuNP surface, one needs to irradiate the AuNPs solution with a laser power density of 1.88 W cm$^{-2}$ for 45 min. We did not further irradiate this sample with power densities below 1.88 W cm$^{-2}$ to avoid too much laser light exposure to the sample and long treatment durations. In addition, we irradiated the other PEGMA@AuNPs solutions with different LCSTs, and the minimum duration times required to change each hydrodynamic diameter at the LCST temperatures are listed in Table 1. In general, except at the laser power density of 0.075 W cm$^{-2}$, there was a hydrodynamic diameter change within 45 min up to the LCST of 69 °C. As expected, the irradiation of higher power densities required shorter durations to change the hydrodynamic diameter of PEGMA@AuNPs.

Figure 5a shows a plot of the laser treatment durations required to change the hydrodynamic diameter of the PEGMA@AuNPs versus different LCST values ranging from 32 °C to 90 °C at different laser power densities. Among the large number of linear, polynomial, power, and exponential functions, the experimental data are best fitted to a high precision seventh-order polynomial function [see Table S1 in the Supporting Information for the fitting parameters, Eq. (1)]. The fitted functions show similar curvatures at all laser power den-

sities (Figure S2 in the Supporting Information). At laser power densities of 1.88 W cm$^{-2}$ and 0.753 W cm$^{-2}$, the time periods needed to change the size of PEGMA@AuNPs are very close to each other up to 55 °C (Figure 5a). Above 55 °C, there is only a relatively slight difference in the required durations for the size change. However, when lower laser power densities of 0.377 and 0.188 W cm$^{-2}$ were used, the durations required for the diameter change of PEGMA@AuNPs become clearer for lower LCST values. It is nearly impossible to reach 75 °C or above by using power densities of 0.377 W cm$^{-2}$ or lower. When using a power density of 0.075 W cm$^{-2}$, only temperatures up to 50 °C were reachable. As a result, from Figure 5a, one can easily calculate the shortest time needed to reach a desired temperature on the AuNP surface upon irradiation of a specific laser power density. Additionally, in a certain time interval, the lowest laser power needed to reach a desired temperature on the Au surface can also be calculated.

The durations required for the hydrodynamic diameter change under laser irradiation versus laser power densities up to 1.88 W cm$^{-2}$ for LCST of PEGMA@AuNPs between 32–79 °C are plotted in Figure 5b by using the data in Table 1. The experimental data are best fitted to quintic/quintic rational functions [see Table S2 in the Supporting Information for the fitting parameters, Eq. (2)]. Fitted functions show similar curvatures at all LCST values (Figure S3 in the Supporting Information) and a parabolic decrease in all LCST values of PEGMA@AuNPs. As expected, the higher the laser power densities are, the shorter the required duration for the change in the hydrodynamic diameter of PEGMA@AuNPs. The duration differences between all these PEGMA@AuNPs decrease and get narrower as higher laser power densities are used. From Figure 5b, one can easily predict the temperature reached on the Au surfaces owing to the photothermal effect of AuNPs at any laser power density below 2 W cm$^{-2}$ at a certain irradiation time.

To generalize our method of measuring the temperature on an AuNP surface, we synthesized a new PEGMA polymer with an LCST of 45 °C (PEGMA45) and then conjugated it to the AuNPs (PEGMA45@AuNPs), which was not used in our previous studies. By using the high precision seventh-order polynomial function fit in Figure 5a, we first calculated the durations required for the hydrodynamic diameter change of PEGMA45@AuNPs upon irradiation with four different laser power densities. The calculated (i.e., theoretical) durations for the size change are 29, 43, 213, and 350 seconds when using 1.88, 0.753, 0.377, and 0.188 W cm$^{-2}$, respectively (plotted in Figure 6). Then, we irradiated the PEGMA45@AuNPs solutions by using the same laser power densities, and similar results of 27, 43, 200, and 360 seconds were experimentally measured as shown in Figure 6. In addition, experimental data for PEGMA45@AuNPs were fitted to a quintic/quintic rational function as in Figure 5b (Figure S4 in the Supporting Information). The calculated times are 26, 46, 198, and 357 seconds for 1.88, 0.753, 0.377, and 0.188 W cm$^{-2}$, respectively. The calculated results using both fit functions show good correlation with experimental results.

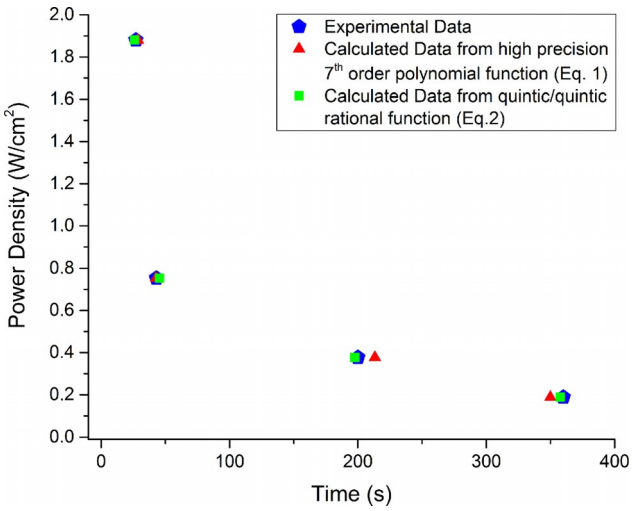


**Figure 6.** Experimental and calculated data of the durations for the changes in hydrodynamic diameters of PEGMA45@AuNP versus power densities of laser.

## Conclusions

We demonstrated a novel strategy to measure the temperature change on the surface of AuNPs during a photothermal process by using a thermoresponsive polymer. This is the first account of a technique to determine the temperature reached or heat generated on Au surfaces at the nanoscale by using prepared thermoresponsive PEGMA polymers. Our results conclude that one can predict more or less accurately how many seconds or minutes are required to reach the desired temperature by using different power densities of CW lasers. The developed PEGMA@AuNPs platform offers a promising background for measuring the temperature generated on the surfaces of various Au nanostructures. We believe that this system would be a very valuable protocol to inspire new designs of thermally responsive platforms, which could lead to easy predictions of the minimum duration needed to destroy cancer cells after optimizing photothermal irradiation conditions in the extracellular matrix and cell medium.

## Experimental Section

### Materials

All the chemicals were used as received. Hydrogen tetrachloroaurate(III) hydrate ($HAuCl_4 \cdot 3H_2O$, 99.9%), trisodium citrate dihydrate ($Na_3C_6H_5O_7 \cdot 2H_2O$, >99%), oligo ethylene glycol methyl ether methacrylate (OEGMA, $M_w = 475$ g mol$^{-1}$), diethylene glycol methyl ether methacrylate (DEGMA, $M_w = 188$ g mol$^{-1}$), 2,2′-bipyridine, and bis(2-hydroxyethyl) disulfide bis(2-bromopropionate) were obtained from Sigma–Aldrich and used as received. Copper bromide (CuBr) was purchased from Alfa Aesar. Dialysis tubes with a nominal molecular weight cutoff of 12 000–14 000 Daltons (Fisherbrand dialysis tubing) were obtained from Fisher Scientific. Distilled water (Sartorius) was used to prepare all aqueous solutions.

### Synthesis of PEGMA polymer by ATRP

The poly(ethylene glycol) methylether methacrylate (PEGMA) polymers were synthesized by using Lutz' method.[20] In a typical reaction, a total volume of 1.5 mL monomers OEGMA ($M_w$ = 475 g mol$^{-1}$), DEGMA ($M_w$ = 188 g mol$^{-1}$), bis(2-hydroxyethyl)disulfide bis(2-bromopropionate) [BHEDS (BP) 2] (8.4 mg), CuBr (3.12 mg), 2,2′-bipyridyl (6.8 mg), and ethanol (0.625 mL) were added into a 4 mL glass vial containing a magnetic stirrer. The polymerization was carried out overnight at room temperature. After polymerization, the product was put into a dialysis bag (molecular cutoff: 12000–14000) and dialyzed at 25 °C for 3 days. All PEGMA polymers with LCST values of 28, 32, 37, 39, 49, 59, 90 °C were synthesized according to the same procedure. New PEGMA polymers with LCSTs 69 and 79 °C were synthesized by using the same procedure and the monomers were added as follows: DEGMA (50%, 0.204 g) and OEGMA (50%, 0.515 g) for LCST at 69 °C; DEGMA (40%, 0.163 g) and OEGMA (60%, 0.618 g) for LCST at 79 °C. Molecular weight values of the polymers with different LCST values (28, 32, 37, 39, 49, 59, 69, 79, and 90 °C) are 48542.7, 51207.1, 48656.8, 52316.1, 64935.4, 48118.2, 50334.7, 62650.7, and 43406.3 g mol$^{-1}$, respectively.

### Synthesis of gold nanoparticles

The 23 nm gold nanoparticles were synthesized by using the Turkevich method,[22] which is as follows: aqueous $HAuCl_4$ solution (1 mL, 12.7 mM) was added to deionized water (49 mL). The mixture was heated to boiling with stirring. Then, trisodium citrate solution (1 mL, 38.8 M) was added to the boiling mixture at once and the mixture was stirred for 15 min. After cooling to room temperature, the samples were centrifuged and washed several times with distilled water to generate citrate-AuNPs.

### Conjugation of PEGMA polymer to the citrate-AuNPs

AuNPs solution (1 mL from 50 mL stock solution) was added to PEGMA polymer (4 mL of 0.3 g) in a 20 mL glass vial. Then, the mixture was shaken overnight at room temperature. PEGMA polymer coated AuNPs were centrifuged at 13300 rpm for 15 min and then the supernatant was discarded. Fresh deionized water was added to the AuNPs and sonicated to disperse the AuNPs. This washing cycle was repeated at least two times more to purify the PEGMA coated AuNPs (PEGMA@AuNPs).

### Determining the hydrodynamic diameter of the PEGMA@AuNPs upon conventional heating or laser irradiation

By using dynamic light scattering (DLS) spectroscopy, the hydrodynamic diameter of the nanostructures can be measured in different temperature environments. The thermoresponsive PEGMA@AuNPs solution (1 mL, $4.27\times10^{12}$ particles mL$^{-1}$) was placed in a DLS cuvette and heated from 28 °C to 90 °C. The changes in the hydrodynamic diameter of solutions upon conventional heating were measured. In the case of laser irradiation, the samples were irradiated with certain laser power densities for a period and then the DLS measurement was immediately recorded.

### Characterization

UV/Vis spectra were recorded by using a Libra S22 spectrophotometer equipped with a temperature controller. To measure the LCST of the thermoresponsive polymer, the permeability of each aqueous polymer solution was monitored by using a UV/Vis Spectrophotometer at a wavelength of 450 nm with each 1 °C increments.[23] Dynamic light scattering (DLS, Nano ZS, Malvern Instruments) was used to determine the average hydrodynamic diameters and polydispersity indexes (PDI) of the synthesized AuNPs, and PEGMA@AuNPs before and after laser irradiation. DLS was applied with an angle of 173° by using a He:Ne laser (4 mW) operated at 633 nm. The PDI values for the size distribution were directly obtained by the software (DTS version 5.10) for hydrodynamic diameter distribution analysis after three consecutive measurements, which is a total of 12 individual runs for each sample. The average hydrodynamic diameters of the nanoparticles were measured in aqueous 10 mM NaCl solutions. Fourier transform infrared (FTIR) spectra (4000–400 cm$^{-1}$) were acquired by using a VERTEX 70 spectrophotometer (Bruker, Germany) at 4 cm$^{-1}$ resolution and 16 scans at room temperature. The relative molecular weights and molecular weight distributions were determined by gel permeation chromatography (GPC) at 25 °C by using a PerkinElmer Series 200 system (100 mL injection column, PL gel 10 mm 300×7.5 mm mixed-B columns, poly(methyl methacrylate) calibration) and dimethyl formamide (DMF) containing LiBr (0.05 mol L$^{-1}$) was utilized as the mobile phase at a flow rate of 1.0 mL min$^{-1}$. A 532 nm continuous-wave visible laser (Changchun New Industries Optoelectronics Technology, Changchun, China; fluence: tunable 0–2.5 W, spot size: 3 mm) was used in laser experiments. A JEOL JEM-2100F 200 kV model transmission electron microscopy (TEM) was used to obtain the TEM images.

### Data fitting procedure

The following procedure was applied to time versus different LCST values of PEGMA-coated AuNPs and time versus power density with respect to the LCST values of PEGMA-coated AuNPs. Experimental data is first fitted to a spline function, which is a series of polynomial functions fitted to sections of the data and knotted to join at points of equal gradient. The spline curve can take any arbitrary curvatures, minimizing unnecessary oscillations, and producing short arcs. Fitted spline functions give a valuable description of the trend but have no value as a model for casual relations. Modeling the casual relations, spline function data was used for a later fitting procedure. Apart from the linear relationship, more than 10000 functions (polynomial, power, exponential, logarithmic, etc.) were evaluated for the best fit. Two constrains were applied to the time domains in the fitting functions: 1) the magnitude of a particular time domain should always be larger than that of the previous one to prevent oscillation, and 2) after 45 min, there should be a sharp increase in time domain (this is an experimental observation). Figure 5a shows a plot of the laser treatment durations required to change the hydrodynamic diameter of the PEGMA@AuNPs versus different LCST values ranging from 32 °C to 90 °C at different laser power densities. The data are best fitted to a high precision seventh-order polynomial function. The durations required for the hydrodynamic diameter change under laser irradiations versus laser power densities up to 1.88 W cm$^{-2}$ for LCST of PEGMA@AuNPs between 32–79 °C are plotted in Figure 5b. The experimental data are best fitted to quintic/quintic rational functions. Besides experimental data, the theoretical data points were inserted to the graphs by using the high precision seventh-order polynomial function or quintic/quintic rational function.

## Acknowledgments

This work was supported by the Research Foundation of the Selcuk University (BAP), Abdullah Gül University (BAP) (Project

No: FOA-2015-9), and TUBITAK (Project No. 112M096, COST TD1004, COST MP1302). Gokhan Demirel acknowledges support from the Turkish Academy of Sciences Distinguished Young Scientist Award (TUBA-GEBIP).

## Conflict of interest

The authors declare no conflict of interest.

**Keywords:** gold nanoparticles · lower critical solution temperature · poly(ethylene glycol) methylether methacrylate · photothermal · thermometers · thermoresponsive polymers

[1] a) X. Yang, M. Yang, B. Pang, M. Vara, Y. Xia, *Chem. Rev.* **2015**, *115*, 10410 – 10488; b) Q. Ban, T. Bai, X. Duan, J. Kong, *Biomater. Sci.* **2017**, *5*, 190 – 210.

[2] a) S. E. Skrabalak, L. Au, X. Lu, X. Li, Y. Xia, *Nanomedicine* **2007**, *2*, 657 – 668; b) H. Ding, D. Yang, C. Zhao, Z. Song, P. Liu, Y. Wang, Z. Chen, J. Shen, *ACS Appl. Mater. Interfaces* **2015**, *7*, 4713 – 4719; c) M. S. Yavuz, Y. Cheng, J. Chen, C. M. Cobley, Q. Zhang, M. Rycenga, J. Xie, C. Kim, K. H. Song, A. G. Schwartz, L. V. Wang, Y. Xia, *Nat. Mater.* **2009**, *8*, 935 – 939.

[3] a) I. H. El-Sayed, X. Huang, M. A. El-Sayed, *Nano Lett.* **2005**, *5*, 829 – 834; b) P. Fortina, L. J. Kricka, D. J. Graves, J. Park, T. Hyslop, F. Tam, N. Halas, S. Surrey, S. A. Waldman, *Trends Biotechnol.* **2007**, *25*, 145 – 152; c) M. Yang, D. Huo, K. D. Gilroy, X. Sun, D. Sultan, H. Luehmann, L. Detering, S. Li, D. Qin, Y. Liu, Y. Xia, *ChemNanoMat* **2017**, *3*, 44 – 50.

[4] a) J. Qiu, W. D. Wei, *J. Phys. Chem. C* **2014**, *118*, 20735 – 20749; b) J. M. Walker, L. Gou, S. Bhattacharyya, S. E. Lindahl, J. M. Zaleski, *Chem. Mater.* **2011**, *23*, 5275 – 5281; c) Y. Wu, D. Su, D. Qin, *ChemNanoMat* **2017**, *3*, 245 – 251.

[5] K. M. Haas, B. J. Lear, *Nanoscale* **2013**, *5*, 5247 – 5251.

[6] a) M. L. Debasu, C. D. S. Brites, S. Balabhadra, H. Oliveira, J. Rocha, L. D. Carlos, *ChemNanoMat* **2016**, *2*, 520 – 527; b) M. Borzenkov, A. Määttänen, P. Ihalainen, M. Collini, E. Cabrini, G. Dacarro, P. Pallavicini, G. Chirico, *ACS Appl. Mater. Interfaces* **2016**, *8*, 9909 – 9916.

[7] a) R. S. Norman, J. W. Stone, A. Gole, C. J. Murphy, T. L. Sabo-Attwood, *Nano Lett.* **2008**, *8*, 302 – 306; b) L. Tong, Y. Zhao, T. B. Huff, M. N. Hansen, A. Wei, J.-X. Cheng, *Adv. Mater.* **2007**, *19*, 3136 – 3141; c) C. Zhu, H.-C. Peng, J. Zeng, J. Liu, Z. Gu, Y. Xia, *J. Am. Chem. Soc.* **2012**, *134*, 20234 – 20237; d) O. Guselnikova, P. Postnikov, Y. Kalachyova, Z. Kolska, M. Libansky, J. Zima, V. Svorcik, O. Lyutakov, *ChemNanoMat* **2017**, *3*, 135 – 144.

[8] C. M. Pitsillides, E. K. Joe, X. Wei, R. R. Anderson, C. P. Lin, *Biophys. J.* **2003**, *84*, 4023 – 4032.

[9] I. H. El-Sayed, X. Huang, M. A. El-Sayed, *Cancer Lett.* **2006**, *239*, 129 – 135.

[10] D. Pissuwan, C. H. Cortie, S. M. Valenzuela, M. B. Cortie, *Gold Bull.* **2007**, *40*, 121 – 129.

[11] M. Fedoruk, M. Meixner, S. Carretero-Palacios, T. Lohmüller, J. Feldmann, *ACS Nano* **2013**, *7*, 7648 – 7653.

[12] K. M. Haas, B. J. Lear, *Chem. Sci.* **2015**, *6*, 6462 – 6467.

[13] Z. Cao, R. Wang, F. Yang, L. Hao, W. Jiao, W. Liu, Q. Wang, B. Zhang, *RSC Adv.* **2015**, *5*, 102167 – 102172.

[14] H. Erdogan, H. Sakalak, M. S. Yavuz, G. Demirel, *Langmuir* **2013**, *29*, 6975 – 6982.

[15] a) J. Chen, C. Glaus, R. Laforest, Q. Zhang, M. Yang, M. Gidding, M. J. Welch, Y. Xia, *Small* **2010**, *6*, 811 – 817; b) S. Kim, A. N. Mitropoulos, J. D. Spitzberg, H. Tao, D. L. Kaplan, F. G. Omenetto, *Nat. Photonics* **2012**, *6*, 818 – 823.

[16] a) H. Zhou, M. Sharma, O. Berezin, D. Zuckerman, M. Y. Berezin, *ChemPhysChem* **2016**, *17*, 27 – 36; b) F. Vetrone, R. Naccache, A. Zamarrón, A. Juarranz de la Fuente, F. Sanz-Rodríguez, L. Martinez Maestro, E. Martín Rodriguez, D. Jaque, J. García Solé, J. A. Capobianco, *ACS Nano* **2010**, *4*, 3254 – 3258; c) G. W. Walker, V. C. Sundar, C. M. Rudzinski, A. W. Wun, M. G. Bawendi, D. G. Nocera, *Appl. Phys. Lett.* **2003**, *83*, 3555 – 3557; d) T. Bai, N. Gu, *Small* **2016**, *12*, 4590 – 4610; e) D. Jaque, B. d. Rosal, E. M. Rodríguez, L. M. Maestro, P. Haro-González, J. G. Solé, *Nanomedicine* **2014**, *9*, 1047 – 1062.

[17] a) S. Ebrahimi, Y. Akhlaghi, M. Kompany-Zareh, Å. Rinnan, *ACS Nano* **2014**, *8*, 10372 – 10382; b) C. P. Kabb, R. N. Carmean, B. S. Sumerlin, *Chem. Sci.* **2015**, *6*, 5662 – 5669; c) T. P. Gustafson, Q. Cao, S. T. Wang, M. Y. Berezin, *Chem. Commun.* **2013**, *49*, 680 – 682.

[18] N. V. Tsarevsky, K. Matyjaszewski, *Macromolecules* **2002**, *35*, 9009 – 9014.

[19] Y. Dong, P. Gunning, H. Cao, A. Mathew, B. Newland, A. O. Saeed, J. P. Magnusson, C. Alexander, H. Tai, A. Pandit, W. Wang, *Polym. Chem.* **2010**, *1*, 827 – 830.

[20] a) J.-F. Lutz, Ö. Akdemir, A. Hoth, *J. Am. Chem. Soc.* **2006**, *128*, 13046 – 13047; b) D. Fournier, R. Hoogenboom, H. M. L. Thijs, R. M. Paulus, U. S. Schubert, *Macromolecules* **2007**, *40*, 915 – 920.

[21] Y. Kotsuchibashi, R. Narain, *Polym. Chem.* **2014**, *5*, 3061 – 3070.

[22] J. Turkevich, P. C. Stevenson, J. Hillier, *Discuss. Faraday Soc.* **1951**, *11*, 55 – 75.

[23] J.-F. Lutz, A. Hoth, *Macromolecules* **2006**, *39*, 893 – 896.

Manuscript received: March 23, 2017
Revised manuscript received: May 8, 2017
Accepted manuscript online: May 10, 2017
Version of record online: June 13, 2017